Biosensors and Bioelectronics 25 (2010) 1240–1243

Contents lists available at ScienceDirect

Biosensors and Bioelectronics

journal homepage: www.elsevier.com/locate/bios

Short communication

Aptamer based surface enhanced Raman scattering detection of vasopressin using multilayer nanotube arrays

Yun Suk Huh, David Erickson*

Sibley School of Mechanical and Aerospace Engineering, Cornell University, Ithaca, NY 14853, USA

ARTICLE INFO

Article history:
Received 6 August 2009
Received in revised form
22 September 2009
Accepted 28 September 2009
Available online 7 October 2009

Keywords:
SERS-active substrate
Nanotube array
Optofluidic device
Aptamer
Vasopressin

ABSTRACT

Here we present an optofluidic surface enhanced Raman spectroscopy (SERS) device for on-chip detection of vasopressin using an aptamer based binding assay. To create the SERS-active substrate, densely packed, 200 nm diameter, metal nanotube arrays were fabricated using an anodized alumina nanoporous membrane as a template for shadow evaporation. We explore the use of both single layer Au structures and multilayer Au/Ag/Au structures and also demonstrate a facile technique for integrating the membranes with all polydimethylsiloxane (PDMS) microfluidic devices. Using the integrated device, we demonstrate a linear response in the main detection peak intensity to solution phase concentration and a limit of detection on the order of 5.2 μU/mL. This low limit of detection is obtained with device containing the multilayer SERS substrate which we show exhibits a stronger Raman enhancement while maintaining biocompatibility and ease or surface reactivity with the capture probe.

© 2009 Elsevier B.V. All rights reserved.

1. Introduction

Surface enhanced Raman scattering (SERS) has recently attracted considerable attention for ultrasensitive, highly specific and low limit of detection biomolecular detection (Braun et al., 2007; Huh et al., 2009a; Jackson and Halas, 2004). The information content and sensitivity of the Raman signal to a large number of common analytes makes SERS particularly attractive for studies of biological systems (Abell et al., 2009; Chen and Choo, 2008; Chou et al., 2008; Driskell et al., 2008; Kim et al., 2009). A key challenge however in the analytical application of SERS is in developing stable and reproducible SERS-active substrates that simultaneously provide a consistent, repeatable and large Raman enhancement factor (Kostovski et al., 2009; Tan et al., 2007).

To address this challenge, several groups have recently developed manufacturing techniques aimed at obtaining homogeneously nanostructured SERS-active substrates (Das et al., 2009; Felidj et al., 2004; Liu and Lee, 2005; Nie and Emory, 1997). Examples of such methods include the use of arrayed nanoparticles (Brolo et al., 2004), metal nanoshells (Jackson and Halas, 2004; Lee et al., 2009), nanorings (Aizpurua et al., 2003) and nanorods (Nikoobakht and El-Sayed, 2003). While these surface phase systems have yielded enhanced uniformity and repeatability of the SERS signal, these approaches can complicate chip fabrication and subsequent integration with microfluidic devices. Integration of SERS-active substrates with microfluidic infrastructure (Anne et al., 2009; Gamby et al., 2009; Liu and Lee, 2005) has a number of advantages including reduced reaction time, potential for multistage automation, and greater signal reproducibility (since the reagents can be delivered more precisely).

Vasopressin (VP) is a peptide hormone that is stored/secreted by the posterior lobe of the pituitary gland. The primary function of VP is to regulate extracellular fluid volume in the body by affecting renal handling of water. In case of patients in hemorrhagic shock, the progression to late phase hemorrhagic shock can be indicated by a marked decrease plasma VP levels (Lienhart et al., 2008; Wenzel et al., 1999). It has also been suggested that replenishing VP can serve to rapidly increase arterial pressure thereby stabilizing the patient (Benrick et al., 2009; Hagler et al., 1985). For example, Krismer et al. (2005) reported a set of human case that injecting dosage of 100–160 IU vasopressin to into human (adults) helped to restore spontaneous circulation. As another experiment, Rusch and Hermsmeyer (1985) demonstrated the effects of vasopressin on membrane potential and tension in isolated segments of basilar arteries by induction of vasopressin concentration (0.01–0.3 IU/mL). As such, VP can be considered both promising biomarker of a critical injury state and a therapeutic agent. We use here an aptamer based binding assay (Purschke et al., 2006; Williams et al., 1997) to perform the VP detection due to the high specificity offered by the approach and the relative ease of generating the recognition agent in comparison with traditional antibodies (Hermann and Patel, 2000).

* Corresponding author. Tel.: +1 607 255 4861; fax: +1 607 255 1222.
E-mail address: de54@cornell.edu (D. Erickson).

0956-5663/$ – see front matter © 2009 Elsevier B.V. All rights reserved.
doi:10.1016/j.bios.2009.09.040

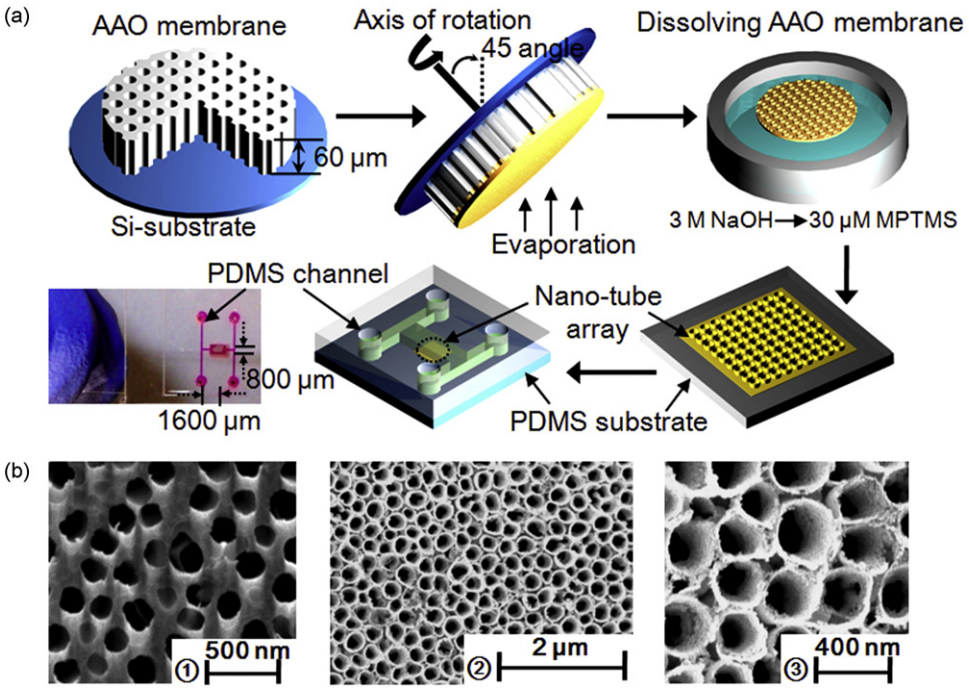

Fig. 1. (a) Schematic of the SERS-active nanotube array fabrication procedure. Anodized alumina (AAO) membrane is attached onto a silicon substrate. After mounting AAO substrate on a rotating chuck, the desired metal structure is deposited onto membrane with an incident 45° angle to the axis of rotation. The metal deposited membrane is then soaked in 3.0 M NaOH for 10 min to dissolve the AAO shadow membrane and yield a metallic nanotube array connected by a continuous backing of the deposited material. After dissolution, the array is dipped in a 30 μM MPTMS solution for 2 h as an organic adhesion layer aiding with the transfer of the nanotube arrays to the PDMS substrate. The enclosed optofluidic chip was then assembled by bonding that substrate with an upper PDMS microfluidic structure fabricated using traditional soft lithography techniques. Final device dimensions are 0.8 mm (width) × 1.6 mm (length). (b) SEM images of (1) bare AAO membrane and (2 and 3) nanotube arrays after dissolving the AAO shadow membrane. The nanotubes formed after evaporation of Au/Ag/Au at an incident angle 45° are about 200 nm diameter and 200 nm height.

The unique SERS substrate we introduce in this paper comprises of ordered nanotube structures which are constructed by metal evaporation through the shadow mask of anodized alumina nanoporous (AAO) membrane. We explore the use of two kinds of SERS-active metal nanotube substrates: a single layer Au structure and a multilayer Au/Ag/Au structure. The latter multilayer structure was designed to in order to take advantage of the greater SERS enhancement offered by the silver while maintaining the biocompatibility and chemical reactivity characteristics (for immobilization of the capture aptamer) offered by the gold outer layer (Malinsky et al., 2001). We also demonstrate a facile assembly technique by which the metallic substrates can be integrated with an all polydimethylsiloxane (PDMS) microfluidic chip.

2. Materials and methods

2.1. Preparation of nanotube arrays

Fig. 1a shows a schematic of the nanotube array fabrication process, which is based on that originally described by Dickey et al. (2008). As shown in Fig. 1a, an AAO membrane (Whatman Anodisc, 60 μm thick, 200 nm diameter pores) was first attached on the topside of a silicon wafer substrate and served as a template for manufacture of the nanotubes during metal evaporation. After the silicon substrate was mounted on a rotating chuck, the Au/Ag/Au metals were sequentially deposited onto the membrane template with an incident 45° angle to the axis of rotation (the same process was used for the single layer structures) at nominal thicknesses of 5 nm, 190 nm and 5 nm respectively. Following this, the metal deposited membrane was immersed in a 3.0 M NaOH for 10 min to dissolve the AAO template yielding the nanotube arrays connected by a continuous backing of the same material. The structures were then dipped in 30 μM 3-mercaptopropyl-trimethoxysilane (MPTMS) solution for 2 h which served as an organic adhesion layer aiding with the transfer of the nanotube arrays onto PDMS. This transfer occurred by allowing the nanotube arrays to gently settle onto the PDMS substrate while gently removing the solution with a syringe. The nanotube coated PDMS substrate was baked at 75 °C for 1 h, rinsed in a DI water overflow chamber for 1 min, and then dried gently with N_2 gas. To bond the nanotube patterned PDMS bottom substrate to the upper PDMS microfluidic system (which was patterned using standard soft lithography techniques) the surfaces of both layers placed in contact after being activated in oxygen plasma.

2.2. Microscopy imaging of nanotube array

For characterization, the bare AAO membrane and the patterned SERS-active PDMS substrate were coated with a Hummer V Au/Pd Sputtering System (Hummer, CA) and imaged with a scanning electron microscope (SEM, Zeiss Ultra/Supra, Germany).

2.3. Aptamer based detection of vasopressin and Raman spectroscopy measurements

Raman measurements were made using an inVia Raman microscope spectrometer coupled to a Leica microscope by focusing the excitation laser on the nanotube arrays. The 488 nm line of an Ar^+ ion laser was used as optical excitation source and the scattered signal was collected by a Peltier-cooled CCD detector. A 50× (NA = 0.55) objective lens was used to focus the laser beam spot onto the sample surface with diameter of about 2 μm. Wave-numbers ranging from 1100 cm^{-1} to 1800 cm^{-1} were examined here.

As mentioned above, in this study VP has been chosen as the target analyte. VP (Arg8-vasopressin) and bovine serum albumin (BSA) were purchased from Sigma (St. Louis, MO, USA). A

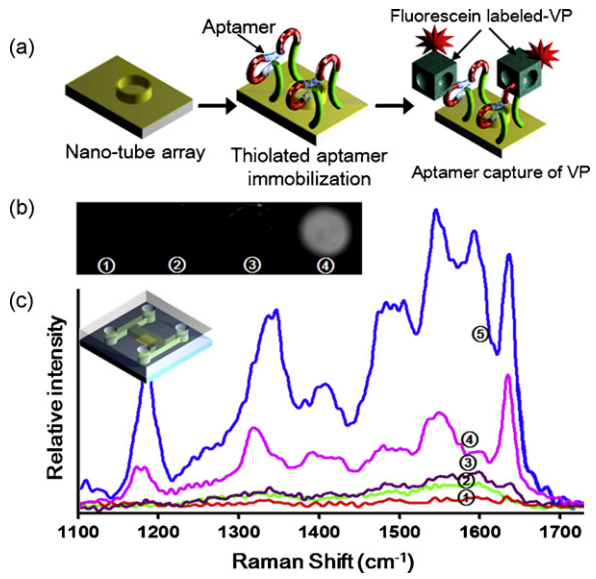

Fig. 2. (a) Schematic of the aptamer–VP recognition binding reaction. (b) Fluorescence images of FITC-labeled aptamer–VP reaction on 200 μm patterned spots under the following conditions (1) background control sample of bare nanotube arrays, (2) after immobilization of the aptamers, (3) after aptamer-BSA reaction (negative control) and (4) after aptamer–VP reaction (positive control). (c) SERS spectra of aptamer–VP reaction corresponding to the first 3 cases described shown in image (b) and (4) for 200 nm Au nanotube arrays and (5) Au/Ag/Au nanotube arrays.

fluorescein labeling Kit (Dojindo, Rockville, MD) was used to functionalize the VP and BSA with a SERS-active dye. Fluorescein labeling technique is mainly used for the preparation of FITC-labeled protein such as BSA and IgG for fluorescence detection (Dalkara et al., 2004; Kulakovich et al., 2006; Pal et al., 2000). The aptamer sequences for VP was 5′ modified with a thiol-modifier containing C_6 S–S functionality and had the following sequence: 5′-S–S–C_6–TCACGTGCATGATAGACGGC GAAGCCGTCG AGTTGCTGTG TGCCGATGCA CGTA (Purschke et al., 2006; Turney et al., 2004). The aptamer sequences were purchased from Integrated DNA Technologies (Operon Biotechnologies, San Diego, CA).

3. Results and discussion

3.1. Fabrication of the nanotube arrays

Fig. 1b shows SEM images of the nanotube arrays manufactured using the techniques described in Section 2.1. The local distribution diameter of nanopore/tube was analyzed using image-analysis software (Scion Image, Scion Corp., Frederick, MD) from the experimental SEM images. In these experiments we used a commercially available AAO membrane which had an average diameter of 209 ± 43 nm (Fig. 1b (1)). After dissolving the AAO template, the resulting SERS-active structure consisted of cylindrical shaped nanotube arrays (15 nm thick and 187 ± 47 nm diameter) as can be seen in Fig. 1b (2) and (3). We believe that this approach represents a more rapid and simple technique to construct SERS-active substrate when compared to more conventional methods such as nanoimprinting (Dana et al., 2008), sputtering method (Zhao et al., 2006), and colloidal lithography methods (Yang et al., 2006).

3.2. Aptamer based SERS detection of vasopressin

For the on-chip assays, we used the well established aptamer-binding assay technique described above and previously in the literature (Purschke et al., 2006; Turney et al., 2004). Fig. 2a shows the schematic of the aptamer–VP binding reaction onto the nanotube structure. As is shown in this figure, after immobilization of the aptamer onto the external gold layer of the SERS substrate, the FITC-labeled VP in PBS buffer solutions were introduced via the inlet port on the microfluidic device. After the reaction was completed, the excitation laser was focused on to the nanotube substrate and the spectrum recorded over an integration time of 15 s. To observe the reaction specificity, the fluorescence intensity of each spot was analyzed (Fig. 2b). As can be seen in curve Fig. 2b (4), strong fluorescence signals were detected in the positive sample at which the FITC-labeled VP had been added. In the negative control experiment, almost no fluorescence signals were detected at the spots of the FITC-labeled BSA. These results suggest that the aptamer-binding assay is a reliable and specific method for detection of VP.

Fig. 2c shows the SERS spectra collected for (1) background control of nanotube array substrate, (2) aptamers immobilized onto the nanotube array, (3) FITC-labeled BSA (negative control), and FITC-labeled VP onto (4) 200 nm Au nanotube arrays and (5) Au/Ag/Au multilayer nanotube arrays. As can be seen in Fig. 2c (3), a small peak around 1600 cm^{-1} was observed from the negative control sample but there are almost no detectable SERS signals beyond 1600 cm^{-1}. For the positive control samples, strong SERS spectra of the FITC-labeled VP are generated. Fig. 2c (4) and (5) show the correct spectroscopic fingerprints corresponding to FITC dye suggesting positive detection (Fabris et al., 2007; Huh et al., 2009b). As mentioned above in order to improve the SERS signal nanotube arrays consisting of different multilayer metallic structures were investigated. As shown in Fig. 2c (4) and (5), the Au/Ag/Au nanotube arrays gave more intense and distinct peaks in all regions of the spectra. As mentioned above this was expected since silver generally provides a much better signal to noise ratio than gold (Yoon et al., 2008). The Raman enhancement factor for the silver nanoparticles is 100–1000 times larger than that that of gold nanoparticles (Chen and Choo, 2008). However, silver has some disadvantages such as biocompatibility, chemical stability, and aggregation properties. To overcome this disadvantage, Park et al. (2009) presented

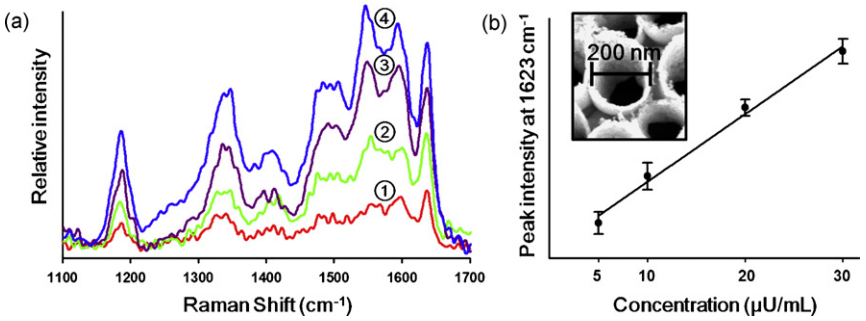

Fig. 3. SERS spectra of FITC-labeled VP bound onto the Au/Ag/Au nanotube arrays at different solution phase concentrations. (1) 5.2 μU/mL, (2) 10.4 μU/mL, (3) 20.8 μU/mL and (4) 31.2 μU/mL. (b) The intensity of SERS signal at 1623 cm^{-1} corresponding to each case illustrated in (a). Error bars indicate standard deviations from three measurements.

the enhancement method of Au/Ag nanostructures for the non-destructive biosensing. By incorporating silver to gold component, the shift of LSPR spectra was greatly increased and the surface immobilization of biomolecules in a non-destructive manner was verified.

To demonstrate the approach for quantitative analysis, we conducted a series of experiments over a range of different VP concentrations. Fig. 3 shows the SERS spectra of FITC-labeled VP onto the multilayer nanotube arrays for various concentrations of (1) 5.2 μU/mL (2) 10.4 μU/mL (3) 20.8 μU/mL and (4) 31.2 μU/mL. For the improvement of the signal to noise of the measurement, we performed the experiment three times to obtain the SERS spectra. As can be seen in Fig. 3b, the intensity of the peak at 1623 cm^{-1} increases linearly with solution phase concentration of the FITC tagged VP, suggesting the technique can be used for quantitative analysis. We thank the reviewer for this comment.

4. Conclusion

In this paper we have demonstrated an optofluidic device for aptamer based VP detection, incorporating a novel metallic multilayer nanotube SERS-active substrate. The nanotubes on SERS-active PDMS substrate are well ordered with uniform packing and an average diameter of 200 nm. With an aptamer based recognition agent we successfully detected SERS signals generated from FITC-labeled vasopressin with a limit of detection on the order of 5.2 μU/mL. In-vivo experiments on the effects of vasopressin were monitored and infused in the vasopressin level of 10 μU/mL to 1000 IU/mL in a continuous or quasi-continuous manner (Hollander et al., 1966; Howl et al., 1999; Krismer et al., 2005). Therefore, this SERS detection system has the sufficient capability to monitor vasopressin levels. We showed that the Au/Ag/Au multilayer nanotube arrays resulted in more intense SERS peaks when compared to single layer Au nanotubes. This simple approach to the creation of regular SERS-active substrates could facilitate future development of miniaturized biomolecular analysis devices.

Acknowledgments

Support for this work was provided by the National Institutes of Health – National Institute of Biomedical Imaging and Bioengineering (NIH-NIBIB) under grant number R21EB007031. The authors also appreciate access and use of the Cornell Nanoscale Science and Technology Facility (a member of the National Nanofabrication Infrastructure Network), which is supported by the National Science Foundation under grant ECS-9731293.

References

Abell, J.L., Driskell, J.D., Dluhy, R.A., Tripp, R.A., Zhao, Y.P., 2009. Biosens. Bioelectron. 24 (12), 3663–3670.
Aizpurua, J., Hanarp, P., Sutherland, D.S., Kall, M., Bryant, G.W., Garcia de Abajo, F.J., 2003. Phys. Rev. Lett. 90 (5), 057401.
Anne, M.Z., Katrin, R.A., Daniell, M., Thomas, B., Thomas, H., Popp, J.G., 2009. J. Biophotonics 2 (4), 232–242.
Benrick, A., Schele, E., Pinnock, S.B., Wernstedt-Asterholm, I., Dickson, S.L., Karlsson-Lindahl, L., Jansson, J.O., 2009. J. Neuroendocrinol. 21 (7), 620–628.
Braun, G., Lee, S.J., Dante, M., Nguyen, T.-Q., Moskovits, M., Reich, N., 2007. J. Am. Chem. Soc. 129 (20), 6378–6379.
Brolo, A.G., Arctander, E., Gordon, R., Leathem, B., Kavanaghs, K.L., 2004. Nano Lett. 4 (10), 2015–2018.
Chen, L., Choo, J., 2008. Electrophoresis 29 (9), 1815–1828.
Chou, I.H., Benford, M., Beier, H.T., Cote, G.L., Wang, M., Jing, N., Kameoka, J., Good, T.A., 2008. Nano Lett. 8 (6), 1729–1735.
Dalkara, D., Zuber, G., Behr, J.-P., 2004. Mol. Ther. 9 (6), 964–969.
Dana, C., Uwe, H.N., Henrik, S., Robert, M.L., Jurgen, P., 2008. Chem. Phys. Chem. 9 (5), 758–762.
Das, G., Mecarini, F., Gentile, F., De Angelis, F., Mohan Kumar, H.G., Candeloro, P., Liberale, C., Cuda, G., Di Fabrizio, E., 2009. Biosens. Bioelectron. 24 (6), 1693–1699.
Dickey, M.D., Weiss, E.A., Smythe, E.J., Chiechi, R.C., Capasso, F., Whitesides, G.M., 2008. ACS Nano 2 (4), 800–808.
Driskell, J.D., Seto, A.G., Jones, L.P., Jokela, S., Dluhy, R.A., Zhao, Y.P., Tripp, R.A., 2008. Biosens. Bioelectron. 24 (4), 917–922.
Fabris, L., Dante, M., Braun, G., Lee, S.J., Reich, N.O., Moskovits, M., Nguyen, T.-Q., Bazan, G.C., 2007. J. Am. Chem. Soc. 129 (19), 6086–6087.
Felidj, N., Truong, S.L., Aubard, J., Levi, G., Krenn, J.R., Hohenau, A., Leitner, A., Aussenegg, F.R., 2004. J. Chem. Phys. 120, 7141–7146.
Gamby, J., Rudolf, A., Abid, M., Girault, H.H., Deslouis, C., Tribollet, B., 2009. Lab Chip 9 (12), 1806–1808.
Hagler, A.T., Osguthorpe, D.J., Dauberosguthorpe, P., Hempel, J.C., 1985. Science 227 (4692), 1309–1315.
Hermann, T., Patel, D.J., 2000. Science 287 (5454), 820.
Hollander, L.P., Franz, J., Berde, B., 1966. Cell. Mol. Life Sci. 22 (5), 325–328.
Howl, J., Prochazka, Z., Wheatley, M., Slaninova, J., 1999. Br. J. Pharm. 128 (3), 647–652.
Huh, Y., Chung, A., Erickson, D., 2009a. Microfluid. Nanofluid. 6 (3), 285–297.
Huh, Y.S., Lowe, A.J., Strickland, A.D., Batt, C.A., Erickson, D., 2009b. J. Am. Chem. Soc. 131 (6), 2208–2213.
Jackson, J.B., Halas, N.J., 2004. Proc. Natl. Acad. Sci. U.S.A. 101 (52), 17930–17935.
Kim, K., Lee, Y.M., Lee, H.B., Shin, K.S., 2009. Biosens. Bioelectron. 24 (12), 3615–3621.
Kostovski, G., White, D.J., Mitchell, A., Austin, M.W., Stoddart, P.R., 2009. Biosens. Bioelectron. 24 (5), 1531–1535.
Krismer, A.C., Wenzel, V., Voelckel, W.G., Innerhofer, P., Stadlbauer, K.H., Haas, T., Pavlic, M., Sparr, H.J., Lindner, K.H., Koenigsrainer, A., 2005. Anaesthesist 54 (3), 220–224.
Kulakovich, O., Strekal', N., Artem'ev, M., Stupak, A., Maskevich, S., Gaponenko, S., 2006. J. Appl. Spectrosc. 73 (6), 892–896.
Lee, S., Chon, H., Lee, M., Choo, J., Shin, S.Y., Lee, Y.H., Rhyu, I.J., Son, S.W., Oh, C.H., 2009. Biosens. Bioelectron. 24 (7), 2260–2263.
Lienhart, H.G., Lindner, K.H., Wenzel, V., 2008. Curr. Opin. Crit. Care 14 (3), 247.
Liu, G.L., Lee, L.P., 2005. Appl. Phys. Lett. 87, 074101.
Malinsky, M.D., Kelly, K.L., Schatz, G.C., Van Duyne, R.P., 2001. J. Am. Chem. Soc. 123 (7), 1471–1482.
Nie, S., Emory, S.R., 1997. Science 275 (5303), 1102–1106.
Nikoobakht, B., El-Sayed, M.A., 2003. J. Phys. Chem. A 107 (18), 3372–3378.
Pal, U., de Silva, A.M., Montgomery, R.R., Fish, D., Anguita, J., Anderson, J.F., Lobet, Y., Fikrig, E., 2000. J. Clin. Invest. 106 (4), 561–569.
Park, K.H., Kim, S., Yang, S.M., Park, H.G., 2009. J. Nanosci. Nanotechnol. 9 (2), 1374–1378.
Purschke, W.G., Eulberg, D., Buchner, K., Vonhoff, S., Klussmann, S., 2006. Proc. Natl. Acad. Sci. U.S.A. 103 (13), 5173–5178.
Rusch, N.J., Hermsmeyer, K., 1985. Ann. Biomed. Eng. 13 (3), 295–302.
Tan, R.Z., Agarwal, A., Balasubramanian, N., Kwong, D.L., Jiang, Y., Widjaja, E., Garland, M., 2007. Sens. Actuators A-Phys. 139 (1–2), 36–41.
Turney, K., Drake, T.J., Smith, J.E., Tan, W., Harrison, W.W., 2004. Rap. Comm. Mass Spectrom. 18 (20).
Wenzel, V., Lindner, K.H., Augenstein, S., Voelckel, W., Strohmenger, H.U., Prengel, A.W., Steinbach, G., 1999. Critical Care Med. 27 (8), 1565.
Williams, K.P., Liu, X.-H., Schumacher, T.N.M., Lin, H.Y., Ausiello, D.A., Kim, P.S., Bartel, D.P., 1997. Proc. Natl. Acad. Sci. U.S.A. 94 (21), 11285–11290.
Yang, S.-M., Jang, S.G., Choi, D.-G., Kim, S., Yu, H.K., 2006. Small 2 (4), 458–475.
Yoon, I., Kang, T., Choi, W., Kim, J., Yoo, Y., Joo, S.-W., Park, Q.H., Ihee, H., Kim, B., 2008. J. Am. Chem. Soc. 131 (2), 758–762.
Zhao, S., Roberge, H., Yelon, A., Veres, T., 2006. J. Am. Chem. Soc. 128 (38), 12352–12353.